

## Optical and Magnetic Studies on ZnO Nanocrystals both Pure and Doped Prepared By Microwave Assisted Solvothermal Method

N. Saraswathi\*, N. Neelakanda Pillai\*\*, C. K. Mahadevan\*

\*(Physics Research centre, S.T.Hindu College, Nagercoil -629 002)

\*\* (Arignar Anna College, Aralvoymoli-629 301)

### ABSTRACT

Nano-structured Zinc oxide is of high potential importance and has wide range of applications. We have made an attempt to investigate the effect of adding  $Mn^{2+}$  and  $S^{2-}$  separately as dopants on the structural, optical, and magnetic properties of nano-structured ZnO. A total of five samples pure and  $Mn^{2+}$  and  $S^{2-}$  added each with two different concentrations viz. 2.5 and 5.0 weight percentages were prepared by a simple, cost-effective, solvothermal method using a domestic microwave oven. The powder X-ray diffraction analysis indicates the hexagonal phase and average grain sizes ranging within 13 to 16 nm. The optical absorption study indicates blue shift on doping. The Photoluminescence spectra indicate violet and bluish green emissions for all the samples studied. The vibration sample magnetometric measurements indicate weak ferromagnetism for all the samples studied.

**Keywords-** Band gap energy, Ferromagnetism, Nanoparticles, Solvothermal, XRD analyses.

### I. Introduction

Nanomaterials have attracted tremendous interest in recent years because of their unique physical and chemical properties, which are highly different from those of either the bulk materials or single atoms [1, 2]. It is a highly challenging work to develop preparation methods that are scalable, cost-effective and environment friendly [3]. Several methods are available for growing nanomaterials in particular ZnO. Some of them are hydrothermal method, atmospheric pressure PVD method, non-hydrolytic route method, wet chemical method and refluxing technique, etc. The simple microwave assisted solvothermal method using a domestic microwave oven is the one we have worked with for the sample preparation.

Growth of transition metal doped wide band gap semiconductors, which show ferromagnetic nature above room temperature is now gaining interest. Nano-structured ZnO (II-VI material) is becoming increasingly important in the present times because of its distinguished properties such as electrical, optical, thermal and magnetic finding potential application as sensors, transducers and

catalysts. Doping, a process by which appropriate elements are introduced into the pure material has

been shown to result in carrier induced ferromagnetism [4,5]. Increase in the dopant concentration can also be increasingly studied because of the effect caused by the defects generated.

Zinc oxide doped with  $Mn^{2+}$  (cationic) and  $S^{2-}$  (anionic) comes under this category after the theoretical work done by Dietl et al [6] who predicted room temperature ferromagnetism in ZnO doped with Mn. Many researchers have also worked in this direction. In the present work, pure and  $Mn^{2+}$  and  $S^{2-}$  doped ZnO nanocrystals were prepared by a simple solvothermal method using a domestic microwave oven and characterized structurally, optically and magnetically. The results obtained are reported herein.

### II. Materials and methods

Analytical Reagent (AR) grade zinc acetate, urea, manganese acetate, thiourea are the precursors and ethylene glycol is the solvent used for the preparation of pure and doped ZnO nanocrystals. Zinc acetate ( $(CH_3COO)_2 Zn \cdot 2H_2O$ ) and urea ( $NH_2 CO NH_2$ ) were taken in 1:3 molecular ratio and dissolved in ethylene glycol and kept in a domestic microwave oven (Frequency = 2.45 GHz and power = 800W). Microwave irradiation was carried out till the solvent was evaporated completely. The colloidal precipitate formed was then cooled and washed several times with double distilled water and with acetone to remove the organic impurities present, if any. The sample was then filtered, dried and collected as yield.

Pure ZnO and ZnO doped with  $Mn^{2+}$  and  $S^{2-}$  (each in two different concentrations, viz. 2.5 and 5 wt %) were prepared. In order to improve ordering the samples were annealed at 400°C for 1 hour. The annealed samples are used for the characterization studies. The mass of the product nanocrystals and the colour of the samples before and after annealing were noted. The yield percentage was calculated using the relation, yield percentage = (Total product mass/Total reactants mass) × 100.

Using an automated X-ray powder diffractometer (PANalytical) with monochromated  $CuK_\alpha$  radiation ( $\lambda = 1.54056\text{\AA}$ ) the powder X-ray diffraction (PXRD) data were collected for all the 5

samples and they were compared with the available literature data for the identification of the sample. Using the Scherrer formula [7] the grain sizes were determined. The prepared samples were subjected to optical and magnetic studies also.

### III. 3.Results and discussions

#### 3.1 General features

The photograph showing the five ZnO samples prepared and also the annealed samples of the same along with the corresponding pellets is provided in Fig 1.

The preparation time, the colour of prepared samples before and after annealing along with the yield percentage are tabulated in Table 1. The yield percentage for the pure sample is about 16.8%. It is higher for the doped samples and is also found to increase with the increase in dopant concentration.

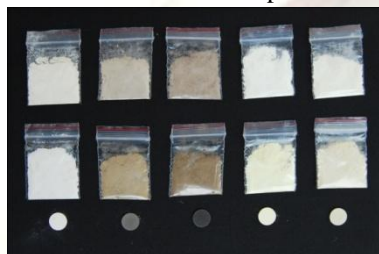


Figure 1: Photograph of the samples prepared

From left: Pure ZnO, ZnO + 2.5 wt % Mn<sup>2+</sup>, ZnO + 5 wt % Mn<sup>2+</sup>, ZnO + 2.5 wt % S<sup>2-</sup>, ZnO + 5 wt % S<sup>2-</sup>

[Top row: As-prepared samples

Middle row: Annealed samples

Bottom row: Pellets of annealed samples]

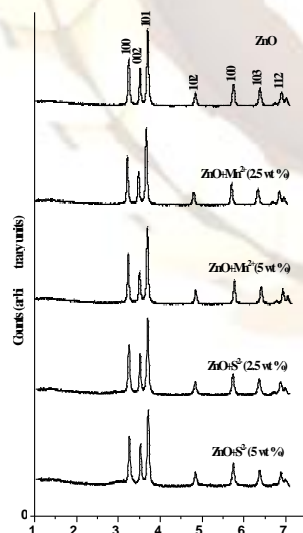


Figure 2: Indexed PXRD patterns for pure and doped ZnO nanocrystals

| (with expected composition)     |      | Before annealing | After annealing       |      |
|---------------------------------|------|------------------|-----------------------|------|
| ZnO                             | 25   | PaleWhite        | White                 | 16.8 |
| ZnO + 2.5 wt % Mn <sup>2+</sup> | 24.5 | Dark paleWhite   | Light yellowish brown | 21.9 |
| ZnO + 5 wt % Mn <sup>2+</sup>   | 22.5 | Light brown      | Brown                 | 23.9 |
| ZnO + 2.5 wt % S <sup>2-</sup>  | 24   | White            | Yellowish white       | 19.3 |
| ZnO + 5 wt % S <sup>2-</sup>    | 22   | White            | Yellowish white       | 20.7 |

Table 1: Preparation times, colours and yield percentages for pure and doped (Mn<sup>2+</sup> & S<sup>2-</sup>) ZnO nanocrystals

The PXRD patterns of the five annealed ZnO samples (both pure and doped) are shown in Figure 2. The peaks obtained matched more appropriately with the hexagonal phase [structure] for Zinc Oxide (JCPDS Card No:36-1451). Almost all the peaks are dominant indicating the crystalline nature of the prepared samples. However, broadening related to size reduction exists. The average grain size of the samples was found by using Scherrer equation :

$$D = \frac{\alpha\lambda}{\beta \cos \theta}$$

where D is the particle size,  $\alpha$  is a constant (0.9),  $\lambda$  is the X-ray wavelength used,  $\theta$  is the Bragg angle and  $\beta$  is the full width at half maximum of diffraction peak (expressed in radian). The lattice parameters a and c estimated by the usual procedure are tabulated in Table 2. It is revealed here that all the prepared ZnO nanocrystals are in the nano regime with average grain size ranging from 13 to 16nm (see Table 2). Amongst the prepared samples the grain size is minimum in the case of ZnO doped with 2.5 wt % S and maximum in the case of the pure sample.

Doping usually causes increase of strains in any material which may be understood by the increase of peak broadening in the spectrum. If strain is not increased then the crystallite size is expected to decrease. Absence of such increase in PXRD peak broadening and slight decrease of crystallite size clearly indicate the non-introduction of any strains in the prepared samples because of doping.

Table 2: The average grain sizes and lattice parameters for pure and doped (Mn<sup>2+</sup> & S<sup>2-</sup>) ZnO nanocrystals

| System | $\bar{D}$ (nm) | Colour | $a$ (Å) | $c$ (Å) |
|--------|----------------|--------|---------|---------|
|--------|----------------|--------|---------|---------|

| System (with expected composition) | Average grain size (nm) | Lattice parameters |        |
|------------------------------------|-------------------------|--------------------|--------|
|                                    |                         | a (Å)              | c (Å)  |
| ZnO                                | 15.70                   | 3.2447             | 5.1958 |
| ZnO + 2.5 wt % Mn <sup>2+</sup>    | 15.01                   | 3.2420             | 5.1883 |
| ZnO + 5 wt % Mn <sup>2+</sup>      | 15.59                   | 3.2448             | 5.1982 |
| ZnO + 2.5 wt % S                   | 13.45                   | 3.4883             | 5.2081 |
| ZnO + 5 wt % S                     | 14.04                   | 3.2462             | 5.1962 |

### 3.2 Optical properties

The UV-Vis absorption spectra were recorded on all the annealed samples. A Shimadzu UV 2400PC spectrophotometer was used. The spectrum which is a plot of the degree of absorption against wavelength of the incident radiation is shown in Fig 3. The wavelength range used for the observation is from 200-1000nm.

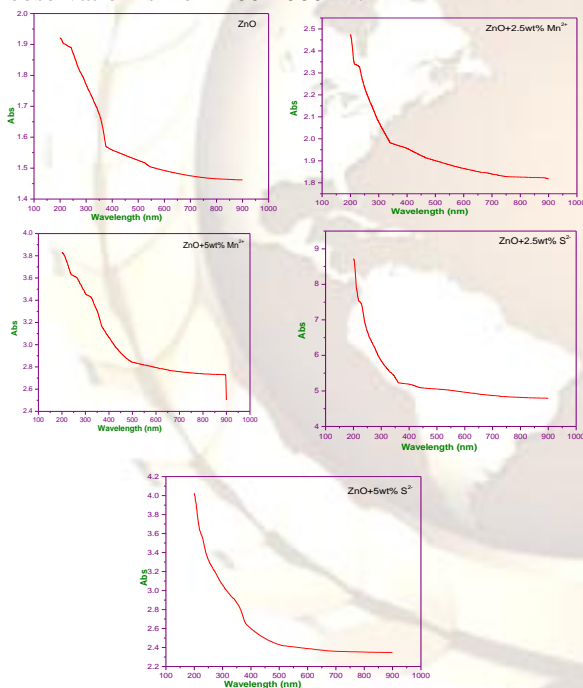


Figure 3: UV absorption spectra for pure and doped ZnO nanocrystal

Major difference in the optical properties of the nanomaterials synthesized is due to the chemical nature of the components. From the spectrum it is evident that ZnO nanocrystals have low absorbance in the visible region. The absorbance first decreases upto 400nm in a steep fashion. Small fluctuations observed may be due to vibrational energy changes that accompany electronic level transitions. If the available energy is insufficient for pure electronic

transitions then they can undergo vibrational transitions from a lower electronic state. The nature of the optical band gap is due to the fundamental absorptions due to electron excitation from the valence band to conduction band.

The band gap energies of the ZnO samples can be found by drawing the  $\alpha(h\nu)$  plots. The band gap energy was estimated in a way as reported by Kumar *et al* [8] and also by Thielsch *et al* [9]. The  $(\alpha h\nu)^n$  versus  $h\nu$  plots for  $n=2, \frac{1}{2}, \frac{1}{3}$  were drawn. The plot showed linear behaviour for  $n=2$  indicating the presence of direct optical band gap in this case. The band gap energy  $E_g$  was found by extrapolating the curve drawn near the absorption edge which is shown in Fig. 4. The band gap energies obtained in this way for ZnO nanocrystals is tabulated in Table 3. The band gap energy is maximum (5.008eV) in the case of ZnO doped with 2.5 wt % S. It is minimum (3.417eV) in the case of pure ZnO. The values for the other samples lie between these two extremes. In the case of doped ZnO increase in the concentration of both the dopants decreases the band gap energy. On analyzing the band gap energy data and average grain sizes calculated from PXRD patterns it can be concluded that increase in band gap energy decreases the grain size of the nanocrystals produced. Quantum confinement may be the agent bringing about increase in band gap energy of the nanocrystal samples.

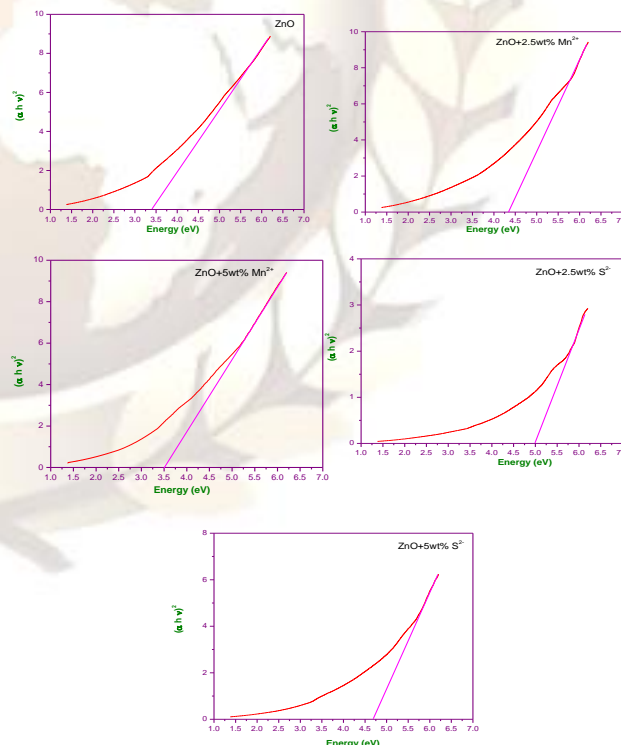


Figure 4:  $(\alpha h\nu)^2$  Vs  $h\nu$  plots for pure and doped ZnO nanocrystals

Table 3: Band gap energies of pure and doped ZnO nanocrystals

| Sample<br>(With estimated composition) | $E_g$ (eV) |
|--|------------|
| ZnO                                    | 3.417      |
| ZnO + 2.5 wt % $Mn^{2+}$               | 4.331      |
| ZnO + 5 wt % $Mn^{2+}$                 | 3.502      |
| ZnO + 2.5 wt % $S^{2-}$                | 5.008      |
| ZnO + 5 wt % $S^{2-}$                  | 4.690      |

When the crystallite size decreases the band gap energy is expected to increase in the case of semiconductor materials indicating a blue shift. In the present study doping has decreased the crystallite size and has increased the optical band gap energy. This is in accordance with the expectation.

The photoluminescence (PL) spectra were recorded for the five annealed ZnO samples using a luminescence spectrometer and analyzed. They are shown in Fig. 5. The samples show two prominent peaks one around 390 nm in the majority of the samples and another around 487 nm. In the case of zinc oxide doped with 2.5wt % of  $Mn^{2+}$  two more peaks are seen around 522 nm and 551 nm. A few other minor peaks are observed in few of the samples. In the case of pure ZnO nanocrystal the peak observed at 394 nm is the intense peak. Incorporation of  $Mn^{2+}$  and  $S^{2-}$  into the ZnO matrix produces changes in the intensity as well as the number of peaks obtained. The peaks obtained may be attributed to the combination of free electrons from the conduction band with holes captured on an acceptor level, recombination of trapped electrons from a donor level with free holes and recombination of electrons from any donor level with holes trapped on an acceptor level [10,11]. The peak around 390 nm corresponds to violet emission peak. The one at 487nm can be attributed to that of bluish green emission peak. Xiying Ma *et al* [12] found a blue emission peak at 432nm for Gd doped ZnO nanocrystals. Romanov *et al* [13] found exciton emission and a blue shift for it while studying ZnO nanocrystals by optically detected magnetic resonance. A strong violet luminescence from ZnO nanocrystals grown by the low temperature chemical solution deposition was shown by Kurbanov *et al* [14]. Wang *et al* [15] studied photoluminescence in ZnO and  $Mg_xZn_{1-x}O$  nanocrystals excited with 290nm light and found two bands, one in the UV region and another in the visible region similar to that of bulk ZnO. Zheng *et al* [16] studied the photoluminescence properties of the Ge/ZnO multilayer films and found green emission at around 532 nm which has been explained. Yang *et al* [17] studied Cu-Zn core alloy and found a green emission around 510 nm and red emission around 650 nm with

PL measurements. Wu *et al* [18] studied room temperature PL spectrum of self-assembly of small ZnO nanoparticles and obtained peaks at 417, 468 and 605 nm.

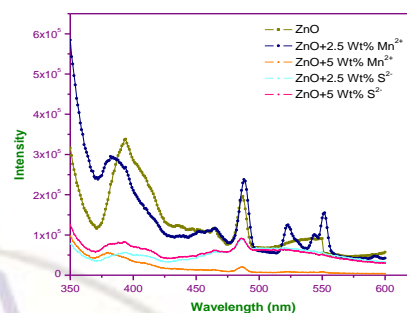


Figure 5: PL spectra for pure and doped ZnO nanocrystals

### 3.3 Magnetic properties

The M-H behaviour of the samples was recorded at room temperature using a vibration sample magnetometer. The M-H plots observed are shown in Fig. 6 and the magnetic parameters are given in Table 4. The samples are found to have a weak ferromagnetic nature that is revealed by the small magnetic hysteresis behaviour shown by the samples. The ferromagnetism can be induced in the sample because of added dopants although they are in very minute amounts. This was observed in the work by Chambers *et al* [19] for ZnO nanocrystals where Co addition brings about changes in its magnetic properties. In the case of ZnO samples coercivity was minimum in the case of ZnO doped with 2.5wt%  $Mn^{2+}$  and maximum in the case of 2.5wt%  $S^{2-}$  added samples. Retentivity and magnetization are found to be maximum in the case of 5wt%  $S^{2-}$  added ZnO nanocrystal. Squareness calculated is maximum for 2.5wt%  $S^{2-}$  doped and minimum for 5 wt%  $Mn^{2+}$  doped ZnO sample. ZnO nanocrystals doped with  $Cr^{3+}$  was studied by Chu *et al* [20] who reported hysteresis behaviour of the sample and also related ferromagnetism. Kshirsagar *et al* [21] studied magnetization as a function of magnetic field for  $Zn_{1-x}Co_xO$  nanocrystals and got a clear hysteresis pattern for  $x = 0.03$ . Oxide nanoparticles are reported [22] to reveal ferromagnetic ordering due to the oxygen vacancies as well. CoO was reported as weakly ferromagnetic [23]. It was also reported that at higher doping concentration the number of magnetic ions is sufficient to render ordered magnetic interaction.

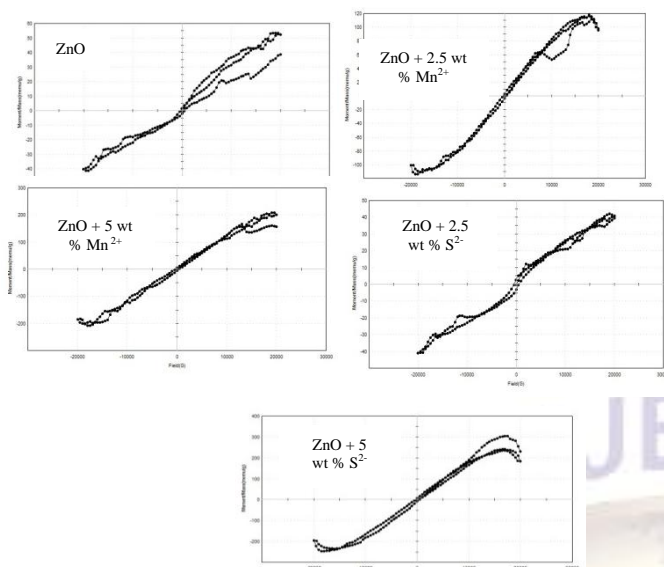


Figure 6: The M-H plots for pure and doped ZnO nanocrystals

Table 4: Results obtained from VSM measurements for the pure and doped ZnO nanocrystals

| System (with expected composition) | Coercivity, $H_c$ (G) | Retentivity, ( $M_r$ ) ( $\times 10^{-6}$ emu) | Magnetization, ( $M_s$ ) ( $\times 10^{-3}$ emu) | Squariness ratio, ( $M_r/M_s$ ) ( $\times 10^{-3}$ ) |
|------------------------------------|-----------------------|--|--|--|
| ZnO                                | 458.3                 | 1.8960   | 0.047454   | 39.950   |
| ZnO + 2.5 wt % $Mn^{2+}$           | 393.73                | 3.6260   | 0.11610  | 31.230   |
| ZnO + 5 wt % $Mn^{2+}$             | 388.06                | 5.2620   | 0.20856  | 25.230   |
| ZnO + 2.5 wt % $S^{2-}$            | 521.31                | 2.8100   | 0.041560   | 67.610   |
| ZnO + 5 wt % $S^{2-}$              | 393.32                | 7.6434   | 0.27600  | 27.690   |

#### IV. Conclusion

Pure and doped ( $Mn^{2+}$  and  $S^{2-}$ ) ZnO nanocrystals were prepared by the simple cost effective microwave assisted solvothermal method using a domestic microwave oven and characterized by PXRD, optical and magnetic measurements. The high yield and the grain sizes observed indicate that the method adopted is a considerable one for the preparation of the nanocrystals studied. The PXRD analysis indicates that all the prepared ZnO nanocrystals are in hexagonal phase structure. When the crystallite size decreases the band gap energy is found to increase which results in the blue shift. In the present study the doping has decreased the crystallite size and has increased the optical band gap energy. The photoluminescence (PL) spectra show

two prominent peaks one around 390 nm and another around 487 nm indicating violet and bluish green emissions. The M-H plots show that the samples are found to have a weak ferromagnetic nature which is revealed by the small magnetic hysteresis behaviour shown by the samples. The ferromagnetism can be induced in the sample because of added dopants although they are in very minute amounts. The present study, in effect, indicates the possible occurrence of nano-confined states.

#### References

- [1] T.Tindade, Nanocrystalline Semiconductors: Synthesis, Properties, and Perspectives, Chem. Mater 13, 2001, 3843-3858.
- [2] A.P.Alivisatos, Semiconductor Clusters, Nanocrystals, and Quantum Dots, Science 271,1996,933-937.
- [3] Z.A. Peng, X.G. Peng, Formation of High-Quality CdTe, CdSe, and CdS Nanocrystals Using CdO as Precursor Z, J.Am.Chem. Soc 123,2001, 183-184.
- [4] Y. Ohno, D. K. Young, B. Beschoten, F. Matsukura, H. Ohno and D. D. Awschalom, Electrical spin injection in a ferromagnetic semiconductor heterostructure, Nature, 402, 1999, 790-791.
- [5] S. J. Pearton, C. R. Abernathy, M. E. Overberg, G. T. Thaler, D. P. Norton, N. Theodoropoulou, A. F. Hebard, Y. D. Park, F. Ren, J. Kim, and L. A. Boatner, Wide band gap Ferromagnetic semiconductors and oxides, J. Appl Phys. 93,2003, 1-13.
- [6] T. Dietl, H. Ohno, F. Matsukura, J. Cibert, and D. Ferrand, Zener Model Description of Ferromagnetism in Zinc-Blende Magnetic Semiconductors, Science, 287, 2000,1019-1022.
- [7] K.U.Madhu, T.H.Freeda and C.K.Mahadevan Preparation and Characterization of ZnO- CdS Quantum Dots, Intl.J. Mater. Sci. 4(5), 2009, 549-556.
- [8] Diwaker Kumar, G.Agarwal, N.Tripathi, D.Vyas and V.Kulshrestha, Characterization of PbS nanoparticles synthesized by chemical bath deposition, J.of Alloys and Comp., 484, 2009, 463-466.
- [9] R.Thielsch, T.Bohme, R.Reiche, D.Schlafer, H.D.Bauer, H.Bottcher, Quantum-size effects of PbS nanocrystallites in evaporated composite films Nano Stru. Mater.,10(2), 1998, 131-149.
- [10] L.S.Pedrotti, D.C.Reynolds, Change in Structure of Blue and Green Fluorescence in Cadmium Sulfide at Low Temperatures, Physical Review 119(6), 1960, 1897-1898.
- [11] B.A.Kulp, H.Kelley Displacement of the Sulfur Atom in CdS by Electron

- Bombardment J Appl. Phys. 31(6), 1960, 1057-1061.
- [12] X.Ma and Z.Wang, The optical properties of rare earth Gd doped ZnO nanocrystals, Mat.Sci. in Semicond. Processing 15(3), 2012, 227-231.
- [13] N.G.Romanov, D.O.Tolmachev, A.G.Badalyan, R.A.Babunts, P.G.Baranov, V.V.Dyakonov, Spin-dependent recombination of defects in bulk ZnO crystals and ZnO nanocrystals as studied by optically detected magnetic resonance, Physica B, 404, 2009, 4783-4786.
- [14] S.S.Kurbanov, G.N.Panin, T.W.Kim, T.W.Kang, Strong violet luminescence from ZnO nanocrystals grown by the low-temperature chemical solution deposition J.of Lumin., 129, 2009,1099-1104.
- [15] Y.S.Wang, ZnO and Mg<sub>x</sub>Zn<sub>1-x</sub>O nanocrystals grown by non-hydrolytic route J. Crys. Growth, 304, 2007, 393-398.
- [16] T.Zheng, Z.Li, J.Chen, K.Shen, K.Sun, Transitions of microstructure and photoluminescence properties of the Ge/ZnO multilayer films in certain annealing temperature region App. Surf. Sci., 252, 2006, 8482-8486.
- [17] N.Yang, H.Yang, Y.Qu, Y.Fan, L.Chang, H.Zhu, M.Li, G.Zou, Preparation of Cu-Zn/ZnO core-shell nanocomposite by surface modification and precipitation process in aqueous solution and its photoluminescence properties Mater. Res. Bull., 41, 2006, 2154-2160
- [18] L.Wu, Y.Wu, Y.Lu., Self-assembly of small ZnO nanoparticles toward flake-like single crystals Mater. Res. Bull., 41, 2006, 128-133
- [19] S.A. Chambers, T.C. Droubay, C.M.Wang, K.M.Rosso, S.M.Heald, D.A.Schwartz, K.R. Kittilsved, D.R. Gamelin Ferromagnetism in oxide semiconductors Materials Today 9(11), 2006, 28-35
- [20] D.Chu, Y.Zeng, D.Jiang, Synthesis and growth mechanism of Cr-doped ZnO single-crystalline nanowires Sol.State Commun.143, 2007, 308-312.
- [21] S.D.Krishsagar, D.Inamder, I.K.Gopalakrishnan, S. K.Kulshreshtha, S. Mahamuni, Formation of room-temperature ferromagnetic Zn<sub>1-x</sub>Co<sub>x</sub>O nanocrystals Sol.State Commun. 143, 2007, 457-460
- [22] A.Sundaresan, R.Bhargavi, N.Rangarajan, U.Siddesh, C.N.R.Rao, Ferromagnetism as a universal feature of nanoparticles of the otherwise nonmagnetic oxides, Phys. Rev.B, 74, 2006, 161306.
- [23] Y.Xiong, L.Z.Zhang, G.Q.Tang, G.L.Zhang, W.J.Chen, ZnO nanoparticles included within all-silica MCM-41: preparation and spectroscopic studies J.Lumin., 110, 2004, 17-22